# Directing the Formation of Nanostructured Rings via Local Oxidation

Andrew Stannard,* Haya Alhummiany, Emmanuelle Pauliac-Vaujour,
James S. Sharp, and Philip Moriarty

*School of Physics and Astronomy, University of Nottingham, University Park, Nottingham NG7 2RD,
United Kingdom*

Uwe Thiele

*School of Mathematics, Loughborough University, Loughborough, Leicestershire LE11 3TU, United Kingdom*

We provide compelling evidence that ring formation in solutions of thiol-passivated Au nanoparticles is driven by breath figure dynamics. A method for the controlled placement of rings of nanoparticles on a solid substrate, which exploits variations in substrate wettability to fix the positions of the submicrometer water droplets formed in the breath figure process, has been developed. This is achieved by heterogeneously patterning hydrogen-terminated silicon substrates with oxide regions that act as adsorption sites for the droplets. The droplets in turn template the formation of thiol-passivated Au nanoparticle rings during spin-casting from volatile solvents.

## I. Introduction

Motivated in part by their unique optoelectronic properties,[1] the fabrication of nanorings has been pursued via many different routes including droplet molecular-beam epitaxy,[2] masked deposition,[3] and templating-based techniques.[4] The rich physics and physical chemistry involved in nanofluid dewetting offers a number of alternative routes toward generating nanoparticle rings on solid substrates, and a rather wide variety of mechanisms have been put forward to explain ring formation during the evaporation of solvent from nanoparticle- or nanorod-containing solutions/suspensions. These span nucleation and expansion of holes in the solvent film,[5−9] the Marangoni effect,[10] periodic contact line pinning and depinning,[11] the formation of gas bubbles in a very thin solvent film,[12] magnetic dipolar interactions,[6] and breath figure formation.[13,14] The latter phenomenon, which exploits the droplets of water that condense on a substrate due to evaporative cooling as templates for nanoring formation, has been used successfully for a range of materials other than nanoparticles/nanorods including single-molecule magnets,[15] polymers (see ref 16 for a review), and hybrid polymer−nanoparticle systems.[17]

When a volume of nanofluid solution is deposited onto a solid substrate, the resulting drying-mediated self-organized morphology of nanoparticles will depend on a range of parameters such as solvent volatility, thin film stability, and interparticle interactions.[18,19] The formation of nanoparticle rings via the creation of holes in a partially wetting volatile thin film has typically been thought of as a three-stage process: nucleation, growth, and arrest. For thin films, the first stage can occur via two mechanisms. Holes can appear homogeneously via thermally driven nucleation without spatial and temporal correlations of the nucleation centers. Alternatively, holes can appear heterogeneously via defect-driven nucleation, resulting in temporal correlations and, thus, rings of similar sizes. Once a hole in the thin volatile film is nucleated, evaporation of solvent from the rim results in a retreat of the substrate−solvent−air contact line; i.e., the hole expands. As the nanoparticles remain in solution, they are collected at the rim. Eventually, growth is arrested and a nanoparticle ring is formed by the deposition of the accumulated nanoparticles.

The origin of the arrest is a slightly contested issue. A continuum model approach by Ohara and Gelbart[5] suggests that the accumulation of particles at the contact line produces an increased frictional force which stops the hole expansion. When this force becomes large enough, hole growth is arrested. This would result in an upper limit to ring size for a given concentration of nanoparticles in solution. A numerical simulation approach by Yosef and Rabani,[7] however, showed that the increased nanoparticle concentration at the rim does not retard the expansion, and hole growth is only arrested via global solvent evaporation. In their model the nanofluid film thins globally via evaporation

*To whom correspondence should be addressed. E-mail: andrew.stannard@nottingham.ac.uk.

(1) Aizpurua, J.; Hanarp, P.; Sutherland, D. S.; Käll, M.; Bryant, G. W.; de Abajo, F. J. G. *Phys. Rev. Lett.* **2003**, *90*, 057401.
(2) Gong, Z.; Niu, Z. C.; Huang, S. S.; Fang, Z. D.; Sun, B. Q.; Xia, J. B. *Appl. Phys. Lett.* **2005**, *87*, 093116.
(3) Larsson, E. M.; Alegret, J.; Käll, M.; Sutherland, D. S. *Nano Lett.* **2007**, *7*, 1256–1263.
(4) Sun, Z.; Li, Y.; Zhang, J.; Li, Y.; Zhao, Z.; Zhang, K.; Zhang, G.; Guo, J.; Yang, B. *Adv. Funct. Mater.* **2008**, *18*, 4036–4042.
(5) Ohara, P. C.; Gelbart, W. M. *Langmuir* **1998**, *14*, 3418–3424.
(6) Tripp, S. L.; Pusztay, S. V.; Ribbe, A. E.; Wei, A. *J. Am. Chem. Soc.* **2002**, *124*, 7914–7915.
(7) Yosef, G.; Rabani, E. *J. Phys. Chem. B* **2006**, *110*, 20965–20972.
(8) Stowell, C.; Korgel, B. A. *Nano Lett.* **2001**, *11*, 595–600.
(9) Stannard, A.; Martin, C. P.; Pauliac-Vaujour, E.; Moriarty, P.; Thiele, U. *J. Phys. Chem. C* **2008**, *112*, 15195–15203.
(10) Maillard, M.; Motte, L.; Pileni, M. P. *Adv. Mater.* **2001**, *13*, 200–204.
(11) Xu, J.; Xia, J.; Lin, Z. *Angew. Chem., Int. Ed.* **2007**, *46*, 1860–1863.
(12) Schenning, A. P. H. J.; Benneker, F. B. G.; Geurts, H. P. M.; Liu, X. Y.; Nolte, R. J. M. *J. Am. Chem. Soc.* **1996**, *118*, 8549–8552.
(13) Khanal, B. P.; Zubarev, E. R. *Angew. Chem., Int. Ed.* **2007**, *46*, 2195–2198.
(14) Zhang, L.; Si, H.-Y.; Zhang, H.-L. *J. Mater. Chem.* **2008**, *18*, 2660–2665.
(15) Gómez-Segura, J.; Kazakova, O.; Davies, J.; Josephs-Franks, P.; Veciana, J.; Ruiz-Molina, D. *Chem. Commun.* **2005**, *45*, 5615–5617.

(16) Bunz, U. H. F. *Adv. Mater.* **2006**, *18*, 973–989.
(17) Böker, A.; Lin, Y.; Chiapperini, K.; Horowitz, R.; Thompson, M.; Carreon, V.; Xu, T.; Abetz, C.; Skaff, H.; Dinsmore, A. D.; Emrick, T.; Russell, T. P. *Nature Mater.* **2004**, *3*, 302–306.
(18) Rabani, E.; Reichman, D. R.; Geissler, P. L.; Brus, L. E. *Nature* **2003**, *426*, 271–274.
(19) Thiele, U.; Vancea, I.; Archer, A. J.; Robbins, M. J.; Frastia, L.; Stannard, A.; Pauliac-Vaujour, E.; Martin, C. P.; Blunt, M. O.; Moriarty, P. J. *J. Phys.: Condens. Matter* **2009**, *21*, 264016.

while the hole is expanding; however, the hole can only expand if the substrate is wet. This predicts no upper size limit as ring size is dictated by the global film thickness when the hole nucleates.

These models of nanoparticle ring formation, however, do not take into account the possibility of water droplets condensing on either the surface of the solvent or on the substrate due to evaporative cooling. There is strong evidence that this so-called "breath figure" effect can play a significant role in the dynamics of ring formation via evaporative dewetting. In particular, Khanal and Zubarev[13] have imaged the formation of a dense array of water microdroplets on the surface of a dichloromethane solution of Au nanorods. Following evaporation of the solvent, a high density of nanorod rings was observed. Zhang et al.[14] have generated impressively ordered arrays of CdSe nanoparticle rings with diameters ranging from 3 $\mu$m to 26 $\mu$m using substrates patterned with microscale checkerboard structures comprising hydrophobic and hydrophilic regions. Water droplets which condensed on the hydrophilic regions again acted as templates for ring formation.

Here we demonstrate the fabrication of nanoparticle rings which are spatially and temporally correlated using an approach which exploits a lithographically defined substrate to template the dewetting of a volatile nanofluid. We use a markedly different technique to that of Zhang et al.,[14] namely, local oxidation of a hydrophobic H:Si(111) surface, to generate nanoscale nucleation sites for ring formation. Our results not only show the central importance of relative humidity, and thus breath figure formation, in ring formation in Au nanoparticle systems but demonstrate that extremely small (~50 nm diameter; ~2 nm high) oxide features are sufficient to determine ring placement.

## II. Experimental Method

In these experiments we used octanethiol ($C_8$) or dodecanethiol ($C_{12}$) passivated 2 nm core diameter Au nanoparticles, synthesized via the Brust et al. technique,[20] and dispersed in one of a number of solvents (toluene, hexane, or dichloromethane) at a concentration of 1 mg/mL. A 25 $\mu$L droplet of this solution was deposited onto a 1 × 1 cm$^2$ square piece of the desired substrate and spin-coated at 4000 rpm to produce a uniform thin film which subsequently thins though evaporative loss of solvent. For some of our experiments (see Results and Discussion) we used a closed spin-coater in which the relative humidity (RH) could be controlled between 20% and 80%. To check the influence of excess surfactant on nanoparticle ring formation, we added 0.1 vol % of octanethiol or dodecanethiol to a number of solutions.

The substrates used were either Si(111) with a native oxide top layer or hydrogen-passivated Si(111) which had been lithographically patterned. H:Si(111) surfaces were patterned via atomic force microscopy (AFM) oxidation[21,22] using an Asylum Research MFP-3D AFM operating in tapping mode (TM). To perform oxide lithography, Pt-coated Olympus AC240 silicon probes where biased to −10 V and scanned across the surface in a 70% humidity environment while using a low set point. The oxide features produced via this method have typical heights and widths of 2 and 50 nm, respectively. After spin-coating the nanofluid solution onto the substrate, samples were then imaged in TM-AFM with the same system using standard Olympus AC240 silicon probes.

## III. Results and Discussion

We focus first on the physical mechanisms underpinning ring formation in Au nanoparticle systems. As briefly outlined in the
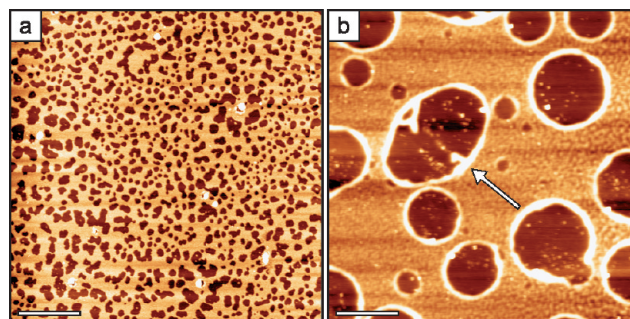


**Figure 1.** Comparison between the morphology of a Au nanoparticle thin film formed by (a) rapid drying of the solvent (dichloromethane) using an argon flow and (b) forced removal of the solvent by breathing on the sample. The arrow in (b) points to a feature which has resulted from the coalescence of two water droplets. Scale bars: 2 $\mu$m.

Introduction, this has been a rather controversial issue with many differing proposals being put forward. The results of a simple initial experiment, however, already point to the key importance of humidity in ring formation. Figure 1 shows TM-AFM images of the morphology of nanoparticle assemblies prepared via two different drying procedures. In both cases, a droplet of $C_{12}$-thiol-terminated Au nanoparticles in dichloromethane was deposited onto a native oxide-terminated silicon substrate inside a Teflon ring using an approach described by Pauliac-Vaujour and Moriarty.[23] For Figure 1a the solvent was rapidly removed by drying with an argon flow, whereas for Figure 1b the dichloromethane was driven off by moist air blown on the sample. (One of the authors simply blew on the surface of the nanoparticle solution.) The difference in the morphology of the resulting nanoparticle films is striking. Blowing the sample with dry gas does not produce any evidence of ring formation whereas removal of the solvent by moist air (i.e., breath) leads to the formation of a high density of rings. We also typically observe many examples of features similar to that highlighted in Figure 1b, whose origin is best explained as arising from the coalescence of water droplets. It is also worth noting that addition of water to the sample surface *following* the preparation of a nanoparticle monolayer similar to that shown in Figure 1a does not produce rings. Instead, and as will be described in detail in a future publication,[24] the two-dimensional nanoparticle monolayer dewets the silicon surface, forming locally thicker (i.e., three-dimensional) regions.

The results of a more controlled experiment are shown in Figure 2. For these measurements we used a sealed spin-coater in which the relative humidity could be controlled between 20% and 80% during spinning of the sample at ~4000 rpm. Identical nanoparticles were used in each case ($C_{12}$-thiol-terminated, ~2 nm core diameter), but they were dissolved in three different solvents—toluene, hexane, and dichloromethane—chosen because of their large range of volatilities (vapor pressures 22, 132, and 353 Torr at room temperature, respectively). As for Figure 1, a native oxide-terminated Si(111) substrate was used.

The top row of Figure 2, i.e. a−c, shows the morphology of the nanoparticle layer formed for spin-casting from toluene under a relative humidity of 10%, 40%, and 70%, respectively. In each case a cellular network structure is formed[25,26] in a layer which is

(20) Brust, M.; Walker, M.; Bethell, D.; Schiffrin, D. J.; Whyman, R. *J. Chem. Soc., Chem. Commun.* **1994**, *7*, 801–802.

(21) Dagata, J. A. *Science* **1995**, *270*, 1625–1626.

(22) Avouris, P.; Hertel, T.; Martel, R. *Appl. Phys. Lett.* **1997**, *71*, 285–287.

(23) Pauliac-Vaujour, E.; Moriarty, P. *J. Phys. Chem. C* **2007**, *111*, 16255–16260.

(24) Alhummiany, H.; Jarvis, S.; Woolley, R. A. J.; Stannard, A.; Blunt, M. O.; Moriarty, P. J., unpublished work.

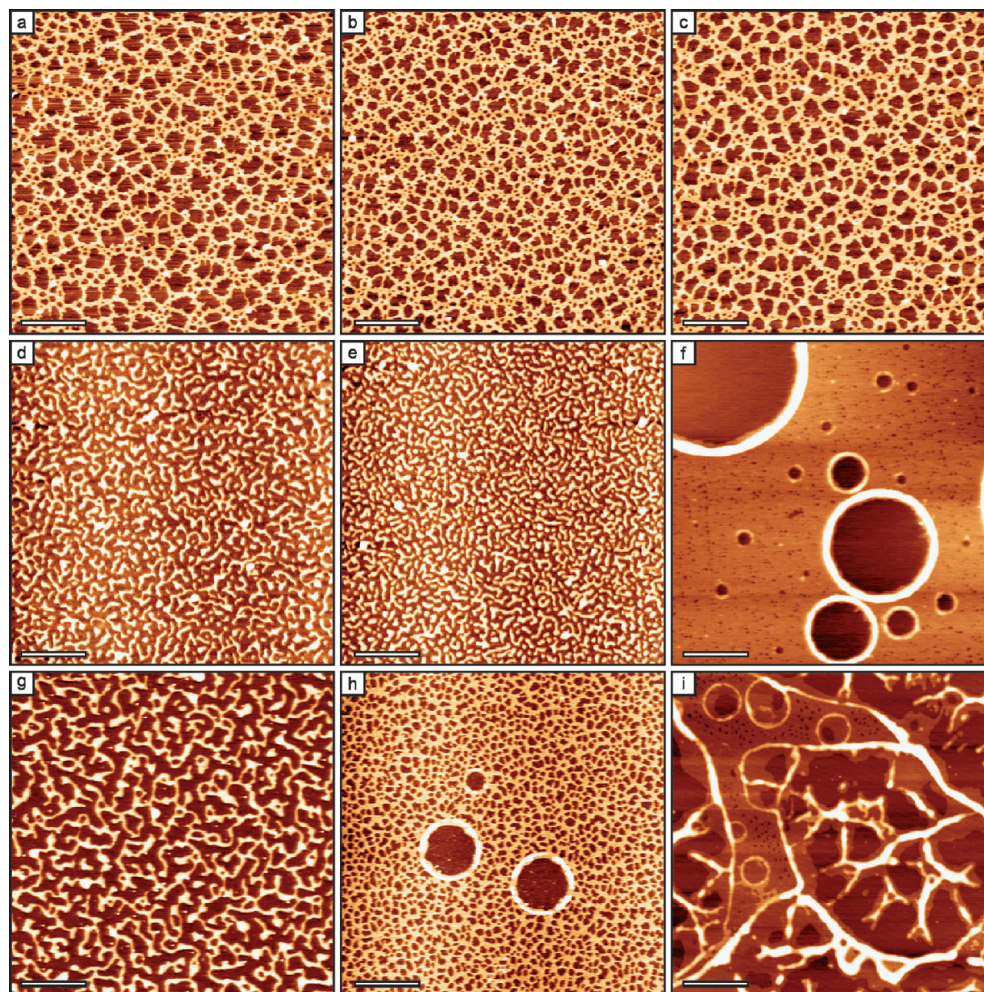(25) Moriarty, P.; Taylor, M. D. R.; Brust, M. *Phys. Rev. Lett.* **2002**, *89*, 248303.

(26) Martin, C. P.; Blunt, M. O.; Moriarty, P. *Nano Lett.* **2004**, *4*, 2389–2392.

**Figure 2.** Effects of the choice of solvent and relative humidity on ring formation in spin-cast Au nanoparticle thin films. The relative humidity varies from 10% (left-hand column) to 70% (right-hand column) while the solvent used was toluene (a−c), hexane (d−f), or dichloromethane (g−i). Solvent volatility thus increases down each column of images. Scale bars: 2 $\mu$m.

one nanoparticle thick. Rings do not form. For hexane (Figure 2d−f) only at higher values of RH (>50%) is ring formation observed (Figure 2f). At smaller values of RH, wormlike domains resulting from spinodal dewetting of the solvent[9,18,27] are formed (Figure 2d,e). Spin-casting from dichloromethane, however, results in ring formation at low RH values (∼30% and above). At a RH of 70% (Figure 2i), the sample morphology is complex and disordered due, most likely, to the formation and coalescence of very many water droplets.

The results of Figure 2 show clearly that *both* a volatile solvent and high RH are required for the formation of rings. (It is interesting to note that for previous work on Au nanoparticle rings hexane[5,10] or chloroform[8] was the solvent used.) The requirement for high RH strongly suggests that the condensation of small water droplets mediates, or templates, the formation of Au nanoparticle rings in a manner akin to that observed for CdSe quantum dots by Zhang, Si, and Zhang.[14] Shah et al.[28] have similarly fabricated highly ordered arrays of holes in Au nanoparticle films via breath figure formation. In that case, however, particles coated with perfluoropolyether were used because dodecanethiol ligands did not sufficiently stabilize the water droplets formed. Although we have not observed the formation of ordered

droplet arrays, our results nonetheless strongly suggest that water condensation can play a significant role in determining the morphology of assemblies and films formed from standard thiol-passivated Au nanoparticles on solid surfaces. Similarly, Ma and Hao[29] have very recently found that porous (honeycomb) films of dodecanethiol-capped Au nanoparticles can be prepared, via breath figure dynamics, at the air/water interface.

To examine the influence of surfactant molecules on the formation of nanoparticle rings, we added excess dodecanethiol (0.1 vol %) to a solution of dodecanethiol-passivated nanoparticles in hexane. The average ring diameter observed following spin-coating at a relative humidity of 70% increased substantially from 1.6 $\mu$m (with a standard deviation of 0.6 $\mu$m) to 3.7 $\mu$m (with a standard deviation of 1.4 $\mu$m). There was also less evidence of droplet coalescence for the solution with excess thiol; i.e., the rings were in general more circular. Excess thiol molecules not only modify the water−solvent interfacial energy but produce a higher nanofluid viscosity.[30] Thus, both the thermodynamics and kinetics of ring formation are affected. The influence of surfactant molecules on breath figure formation in polymer solutions has been studied by Fukuhira et al.,[31] who found that the stability of water

(27) Ge, G.; Brus, L. *J. Phys. Chem. B* **2000**, *104*, 9573–9575.
(28) Shah, P. S.; Sigman, M. B.; Stowell, C. A.; Lim, K. T.; Johnston, K. P.; Korgel, B. A. *Adv. Mater.* **2003**, *15*, 971–974.
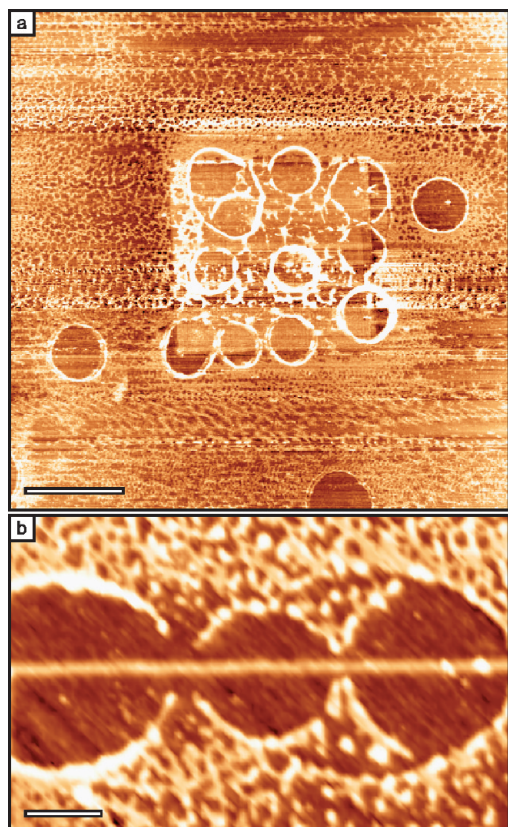(29) Ma, H.; Hao, J. *Chem.—Eur. J.* **2010**, *16*, 655–660.
(30) Pauliac-Vaujour, E.; Stannard, A.; Martin, C. P.; Blunt, M. O.; Notingher, I.; Moriarty, P. J.; Vancea, I.; Thiele, U. *Phys. Rev. Lett.* **2008**, *100*, 176102.
(31) Fukuhira, Y.; Yabu, H.; Ijiro, K.; Shimomura, M. *Soft Matter* **2009**, *5*, 2037–2041.

**Figure 3.** TM-AFM images of nanoparticles deposited from dichloromethane onto patterned substrates. (a) An oxide square, of side length 4 $\mu$m, produces an area where there is a significantly higher density of nanoparticle rings than for the surrounding hydrophobic H:Si(111) surface (scale bar: 2 $\mu$m). (b) An oxide line, ~50 nm width, also leads to the formation of nanoparticle rings (scale bar: 500 nm).

droplets, and thus the structure of the associated breath figure patterns, were strongly affected by the choice of surfactant. Our results for Au nanoparticle solutions indicate that excess surfactant plays a similarly important role in determining the geometry of the rings.

Figure 3a shows a TM-AFM image of the result of nanoparticles dispersed in dichloromethane spin-coated onto an H:Si(111) substrate which has been patterned with a 4 × 4 $\mu$m$^2$ square of oxide. It is clear that the oxide region comprises many nucleation centers for the growth of nanoparticle rings. These nucleation centers are very close together, which necessarily results in the coalescence of the water droplets which have condensed there, thereby producing what are perhaps best described as interpenetrating rings. The presence of many nucleation centers within the patterned region is most likely due to the known poorer quality of lithographically grown oxide, compared to oxide formed under more conventional circumstances. While rings are also observed on the hydrogen-terminated regions, these can be attributed to point defects arising from improper hydrogen passivation or the early stages of substrate reoxidization. In general, rings are most clear on the edges of the square. This may be due to the high wettability gradient associated with the variation in substrate chemistry.[32]

(32) Konnur, R.; Kargupta, K.; Sharma, A. *Phys. Rev. Lett.* **2000**, *84*, 931–934.
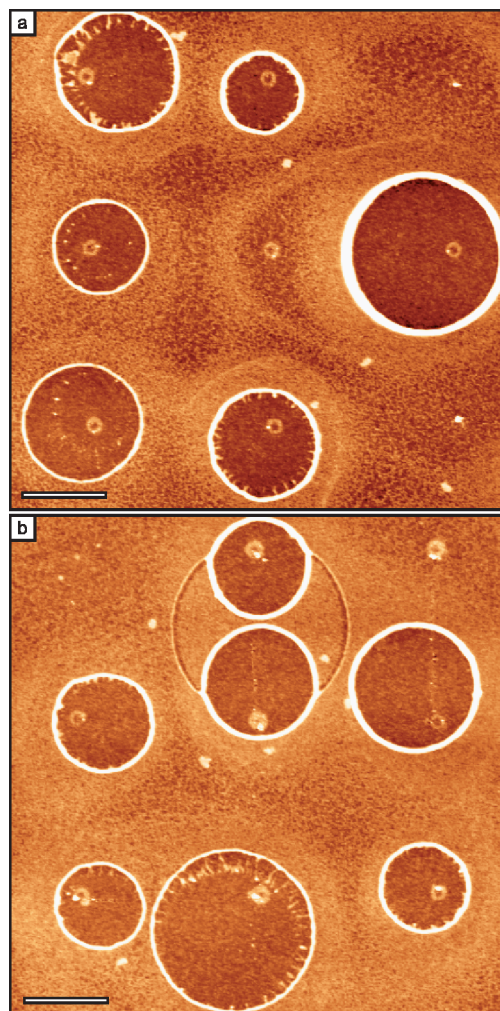


**Figure 4.** TM-AFM images of nanoparticle rings resulting from spin-coating nanoparticles dispersed in dichloromethane onto H:Si(111) substrates lithographically patterned with oxide dots. Scale bars: 1 $\mu$m.

We then patterned a substrate with a quasi-1D feature— a line—to reduce the nucleation density in an attempt to observe more complete, isolated rings. This is shown in Figure 3b where an oxide line has nucleated the formation of a number of nanoparticle rings. The noncircular geometry of the rings may arise either from droplet coalescence or from an anisotropy in the contact line velocity due to the one-dimensional nature of the oxide feature.

The dimensionality of the oxide features was then reduced further, to quasi-0D structures (i.e. dots), to explore their effect on ring formation. Figure 4 shows two TM-AFM images of nanoparticle rings formed via oxide dots. Both of the dot patterns shown here are 3 × 3 arrays where adjacent dots are separated by 2 $\mu$m (the lithographic process was not, however, 100% successful, in that not all dots were drawn properly). The oxide dots, however, produce rings with a high success ratio (just 2 out of 15 dots did not lead to the formation of a ring).

Importantly, the oxide dots tend not to be in the center of the nanoparticle rings. This is an intriguing effect and highlights the complex dynamics underpinning ring formation. Although a detailed understanding of the dynamics currently eludes us (and will therefore be the focus of a future series of experiments using contrast-enhanced optical microscopy[30] to monitor the formation and evolution of micrometer-scale rings), the development of a

ring involves the following four steps at a minimum: (i) nucleation of a hole in the solvent−nanoparticle film, induced by the presence of the oxide dot; (ii) condensation and growth of a water droplet at the position of the dot *or* the movement of a water droplet formed on top of the solvent to the nucleation site via thermocapillary/Marangoni forces; (iii) trapping of nanoparticles at the water−solvent−air three-phase region; and (iv) evaporation of dichloromethane and water. These processes are coupled—indeed, as described below, step ii could plausibly occur before step i—and the dynamics of ring formation will be determined by the local surface/interface tension (influenced by the concentration of nanoparticles and excess surfactant), the respective rates of solvent and water evaporation, solutal and temperature gradient-driven Marangoni convection, and pinning at the substrate.

We can identify a number of features of the experimental setup which provide some insight into the ring formation mechanism. First, our observation that small oxide features (∼2 nm high) can be used to "pin" rings to the substrate strongly suggests that water condensation occurs on thin, rather than thick, solvent films and involves a water/solvent/substrate contact line. It is also worth noting that the solvent layer in a water/solvent/silicon system is inherently less stable than that in an air/solvent/silicon combination. This can be seen from the form of the dielectric response function, $\varepsilon(i\xi)$, for the various materials. In the nonretarded approximation for the interface potential, the interaction of material 1 (i.e., air or water) with material 3 (in our case, silicon (or, more correctly, a silicon dioxide/silicon combination) across material 2 (the solvent) may be described as the sum of terms of the form $-(\varepsilon_1 - \varepsilon_2)(\varepsilon_3 - \varepsilon_2)$; the more negative the value, the more unstable the combination. If the top layer (i.e., material 1) is water, then its highly polar nature, as compared to the organic solvents used in our work, produces a much less stable solvent film. Hence, the condensation of water will destabilize a solvent film on a silicon substrate.

As described by Mahadevan, Add-Bedia, and Pomeau,[33] a droplet comprising two immiscible liquids (such as the organic solvent and water involved in our experiment) can give rise to a number of different configurations: one liquid encapsulates the other with two separate contact lines, one liquid encapsulates the other with merged contact lines, or one liquid forms a droplet on the other liquid such that there is a contact line at the substrate and one at the interface of the liquids. In principle, we could distinguish between these configurations on the basis of surface and interfacial energies of the silicon/silicon oxide/solvent/water/air combination. However, in practice, we cannot use the surface/

interface energy associated with the solvent alone for this calculation as the high concentration of nanoparticles (and excess surfactant) at the water−solvent−substrate contact line will dramatically influence the local contact angle. Moreover, our experiments involve inhomogeneous, rather than homogeneous, substrates where we have deliberately engineered a wettability gradient.

A key contribution to the off-center placement of the rings is likely to be that the solvent−nanoparticle film, already destabilized by the presence of water, will dewet where the wettability gradient is highest,[32] i.e., at the edge of the oxide feature. The oxide feature will also locally pin the solvent−water−substrate contact line, strongly affecting the velocity of the dewetting front. Variations in front velocity are suggested by the nonradially symmetric nanoparticle fingering observed within many of the rings (see, for example, the ring in the top left-hand corner of Figure 4a or that in the middle of the bottom row of Figure 4b). Finger formation in nanoparticle solutions has previously been understood as arising because the velocity of the dewetting front—which is receding by convection and evaporation—is so high that nanoparticles cannot remain solvated at the retreating front. This leads to fingers that are deposited perpendicular to the front.[19,30,34,35] However, fingering instabilities have also been observed for water layers (albeit on much larger length scales) during the formation of porous polystyrene films via a breath figure-related mechanism.[36] Quite what role the condensed water droplet plays in the fingering instability remains an open question which we will address in future work.

## IV. Conclusions

We have shown that relative humidity plays a key role in ring formation in dewetting solutions of thiol-passivated Au nanoparticles. Condensed water droplets act as templates for nanoparticle rings, and thus, variations in substrate wettability—via the local oxidation of H:Si(111)—can be exploited to "pin" rings at specific locations on a solid surface.

(33) Mahadevan, L.; Adda-Bedia, M.; Pomeau, Y. *J. Fluid Mech.* **2002**, *451*, 411–420.

(34) Vancea, I.; Thiele, U.; Pauliac-Vaujour, E.; Stannard, A.; Martin, C. P.; Blunt, M. O.; Moriarty, P. J. *Phys. Rev. E* **2008**, *78*, 041601.
(35) Archer, A. J.; Robbins, M. J.; Thiele, U. *Phys. Rev. E* **2010**, *81*, 021602.
(36) Cai, Y.; Zhang Newby, B. *Langmuir* **2009**, *25*, 7638–7645.